Neuron
Article

Enhancement of Learning and Memory by Elevating Brain Magnesium

Inna Slutsky,[3,6,7] Nashat Abumaria,[1,7] Long-Jun Wu,[5] Chao Huang,[1] Ling Zhang,[1] Bo Li,[1] Xiang Zhao,[1] Arvind Govindarajan,[2,3,4] Ming-Gao Zhao,[5] Min Zhuo,[5] Susumu Tonegawa,[2,3,4] and Guosong Liu[1,3,4,*]
[1]Center for Learning and Memory, School of Medicine, Tsinghua University, Beijing 100084, China
[2]Howard Hughes Medical Institute
[3]Department of Brain and Cognitive Sciences
[4]Department of Biology
Massachusetts Institute of Technology, Cambridge, MA 02139, USA
[5]Department of Physiology, Faculty of Medicine, University of Toronto, Toronto, ON M5S 1A8, Canada
[6]Department of Physiology and Pharmacology, Faculty of Medicine, Tel Aviv University, Tel Aviv 69978, Israel
[7]These authors contributed equally to this work
*Correspondence: liu.guosong@gmail.com
DOI 10.1016/j.neuron.2009.12.026

SUMMARY

Learning and memory are fundamental brain functions affected by dietary and environmental factors. Here, we show that increasing brain magnesium using a newly developed magnesium compound (magnesium-L-threonate, MgT) leads to the enhancement of learning abilities, working memory, and short- and long-term memory in rats. The pattern completion ability was also improved in aged rats. MgT-treated rats had higher density of synaptophysin-/synaptobrevin-positive puncta in DG and CA1 subregions of hippocampus that were correlated with memory improvement. Functionally, magnesium increased the number of functional presynaptic release sites, while it reduced their release probability. The resultant synaptic reconfiguration enabled selective enhancement of synaptic transmission for burst inputs. Coupled with concurrent upregulation of NR2B-containing NMDA receptors and its downstream signaling, synaptic plasticity induced by correlated inputs was enhanced. Our findings suggest that an increase in brain magnesium enhances both short-term synaptic facilitation and long-term potentiation and improves learning and memory functions.

INTRODUCTION

The pattern and strength of synaptic connections are widely believed to code memory traces. Long-term potentiation of synaptic strength (LTP) is correlated with behaviorally relevant memory function: reductions in LTP cause memory impairments (Barnes, 1979; Morris et al., 1986), whereas increases in LTP are associated with enhancement of learning and memory (for reviews, see Lee and Silva, 2009; Martin et al., 2000; Nakazawa et al., 2004). However, the ability to store new information in neural networks depends on the degree of plasticity of synaptic connections, as well as the number of available connections. Therefore, number of synapses should be critical for learning and memory too. Indeed, loss of synapses is correlated with age-dependent memory decline in rats (for review, see Burke and Barnes, 2006; Chen et al., 1995; Smith et al., 2000; Wilson et al., 2006), while hormones and neuropeptides, such as estrogen (Li et al., 2004), neurotophins (Vicario-Abejón et al., 2002), insulin/IGF (Lichtenwalner et al., 2001; O'Kusky et al., 2000), and ghrelin (Diano et al., 2006), increase synaptic density and improve memory.

Diet, in conjunction with environmental factors, has a crucial role in shaping brain cognitive capacity (for review, see Gómez-Pinilla, 2008). Therefore, searching for dietary components that can increase the number and plasticity of synapses might yield new strategies to enhance learning and memory functions. Magnesium (Mg^{2+}), the fourth most abundant ion in body and a cofactor for more than 300 enzymes, is essential for the proper functioning of many tissues and organs, including the cardiovascular, neuromuscular, and nervous systems. In brain, one major action of Mg^{2+} is modulating the voltage-dependent block of NMDA receptors (NMDAR), controlling their opening during coincidence detection that is critical for synaptic plasticity (Mayer et al., 1984; Nowak et al., 1984). Our previous study suggests that Mg^{2+} is a positive regulator of synaptic plasticity; increasing Mg^{2+} concentration in the extracellular fluid ($[Mg^{2+}]_o$) within the physiological range leads to permanent enhancement of synaptic plasticity in networks of cultured hippocampal neurons in vitro (Slutsky et al., 2004). Therefore, it is tempting to investigate whether the increase in brain Mg^{2+} content will enhance cognitive function in vivo.

Mg^{2+} concentration is higher in the cerebrospinal fluid than in plasma. This concentration gradient is maintained by active transport process, which appears to regulate and limit the amount of Mg^{2+} that can be loaded into the brain. In fact, increasing plasma $[Mg^{2+}]$ by 3-fold via intravenous infusion of $MgSO_4$ for 5 days fails to elevate brain Mg^{2+} content in rats (Kim et al., 1996). In human, dramatic increase (100%–300%) in blood $[Mg^{2+}]$ via intravenous infusion of $MgSO_4$ corresponds to elevation in cerebrospinal fluid $[Mg^{2+}]$ only by 10%–19% (McKee et al., 2005). Therefore, boosting brain Mg^{2+} via chronic oral magnesium supplement, the necessary condition for testing the influence of elevating brain

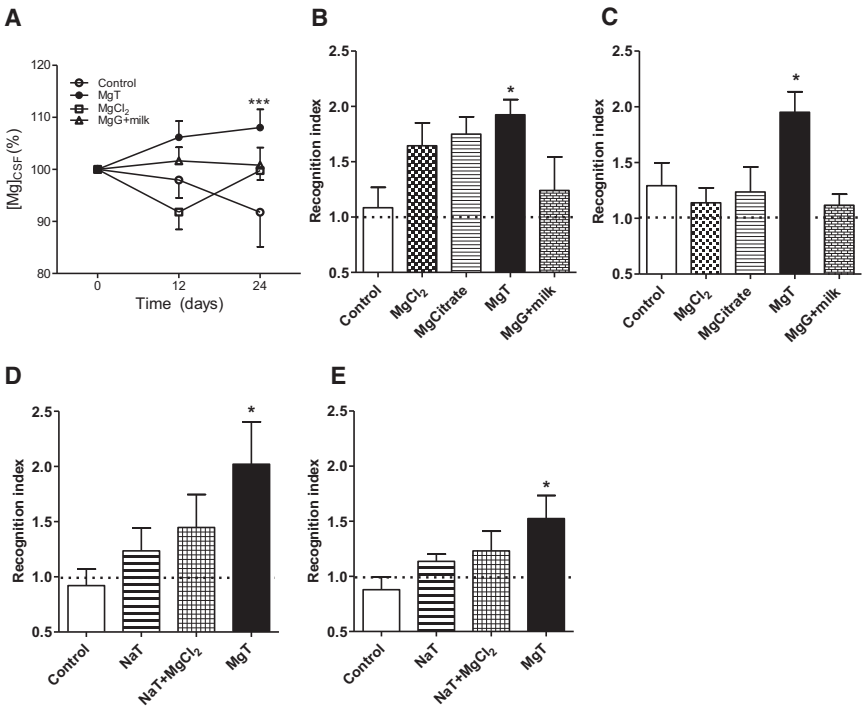

Figure 1. Effect of Various Mg^{2+} Compounds on $[Mg^{2+}]_{CSF}$ and Recognition Memory

(A) Elevation of magnesium concentration in the cerebrospinal fluid ($[Mg^{2+}]_{CSF}$) following treatment with different magnesium compounds. Total Mg^{2+} in CSF was measured before magnesium treatment (day 0), 12, and 24 days after magnesium treatment. Two-way ANOVA analysis revealed significant effect of treatment ($F_{3,69}$ = 4.76, p = 0.0045, n = 6–8). Data were calculated and presented as a percentage of baseline level.

(B) Rat performance during a short-term memory test (10 min retention interval) evaluated by novel object recognition test.

(C) Long-term memory test (12 hr) using novel object recognition test. One-way ANOVA analysis revealed significant effect of treatment on short-term memory ($F_{4,34}$ = 2.89, p = 0.037, n = 7–9) and long-term memory ($F_{4,31}$ = 4.50, p = 0.005, n = 5–10). Post hoc test revealed significant effect of magnesium-L-threonate (MgT) on short term and long-term memory.

(D and E) Effects of sodium-L-threonate (NaT) alone and when combined with magnesium chloride ($MgCl_2$) on short-term memory (D) and long-term memory (E). ANOVA analysis revealed a significant effect of treatment on short-term memory ($F_{3,33}$ = 2.90, p = 0.049, n = 8–10) and long-term memory ($F_{3,34}$ = 3.23, p = 0.034, n = 9–10). Post hoc test revealed significant effect of magnesium-L-threonate (MgT). See also Figures S2 and S3. A modified version of novel object recognition test was used to increase the difficulty of the task (see Supplemental Experimental Procedures and Figure S4). Dashed line indicates no memory. MgG, magnesium gluconate. Bonferroni's post hoc test, *p < 0.05, ***p < 0.001. Data are presented as mean ± SEM.

Mg^{2+}on memory function, is even more challenging. Therefore, we developed a new, highly bioavailable Mg^{2+} compound (magnesium-L-threonate, MgT; for chemical structure, see Figure S1 available online), that could significantly increase Mg^{2+} in the brain via dietary supplementation.

Here, we tested in vivo whether an increase in brain Mg^{2+} by MgT could positively influence learning and memory functions in rats at different ages. We found that elevation of brain Mg^{2+} led to significant enhancement of spatial and associative memory in both young and aged rats. To understand the molecular mechanisms underlying MgT-induced memory enhancement, we studied the changes in functional and structural properties of synapses in rats treated with MgT. The NR2B-containing NMDAR was increased, resulting in enhancement of NMDAR signaling and synaptic plasticity. At the cellular level, the number of presynaptic boutons was also increased. We propose that these positive changes in synaptic functions are the principal cellular mechanisms underlying the enhancement of learning and memory associated with the increase in brain Mg^{2+} content. Thus, elevating brain Mg^{2+} content via increasing magnesium intake might be a useful strategy to enhance cognitive abilities and prevent the age-dependent memory decline.

RESULTS

Identification of Suitable Magnesium Compound for Memory Enhancement

To study the effect of elevating brain Mg^{2+} on learning and memory, we needed to identify a suitable Mg^{2+} compound that enhances loading of Mg^{2+} into the brain. To achieve this goal, the Mg^{2+} compound needs high efficacy to transport Mg^{2+} from the digestive tract into the blood and, ultimately, into the central nervous system. In a separate study, the bioavailability (evaluated by absorption, excretion, and retention rate of magnesium) of four commercially available Mg^{2+} compounds (magnesium-chloride, -citrate, -glycinate, and -gluconate) and two Mg^{2+} preparations we developed (magnesium-L-threonate, MgT, and magnesium-gluconate in milk) was compared in rats. We found that both MgT and magnesium-gluconate in milk have higher bioavailability (X.Z., F. Mao, Y. Shang, N.A., and G.L., unpublished data).

Here, we explored the ability of our newly developed compounds to increase the cerebrospinal fluid (CSF) Mg^{2+} concentration ($[Mg^{2+}]_{CSF}$). CSF was collected before treatment to determine the baseline $[Mg^{2+}]_{CSF}$ of each individual rat. The CSF was then collected 12 and 24 days after magnesium treatment from the same rats. Total $[Mg^{2+}]_{CSF}$ increased gradually in MgT-treated rats. At day 24, $[Mg^{2+}]_{CSF}$ was 7% higher than baseline (one-way ANOVA, p < 0.05, Figure 1A). To monitor the effect of repeated CSF sampling on $[Mg^{2+}]_{CSF}$, we measured $[Mg^{2+}]_{CSF}$ in control rats without any magnesium supplementation. $[Mg^{2+}]_{CSF}$ dropped by ~9% at the third sampling point (24 days, Figure 1A). This drop might be due to the loss of CSF Mg^{2+} associated with CSF sampling; as the CSF volume in rat brain is about 300–400 μl, each sampling (50-100 μl) can lead to 15%–30% loss of CSF Mg^{2+}. Considering this reduction of $[Mg^{2+}]_{CSF}$ associated with the repeated sampling, the actual increase in $[Mg^{2+}]_{CSF}$ should be ~15% (two-way ANOVA,

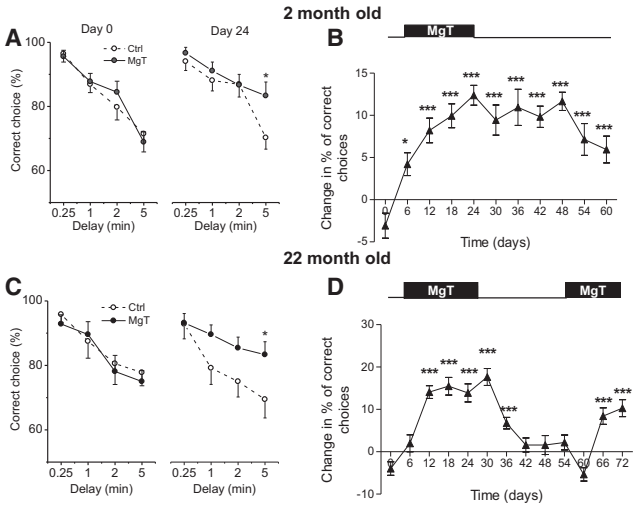

Figure 2. Enhancement of Spatial Working Memory by MgT

(A) Spatial working memory of young rats (2 months) in the T-maze before (day 0) and after (day 24) MgT treatment. MgT-treated rats showed significant improvement in performance at 5 min delay as a retention interval compared to control rats (unpaired t test, *p < 0.05, n = 12). Fifty percent of correct responses represent chance levels of performance. (C) Spatial working-memory of aged rats (22 months) in the T-maze before (day 0) and after (day 24) MgT treatment. MgT-treated rats showed significant improvement in performance after 5 min delay as a retention interval compared to control rats (t test, $p < 0.05$, $n = 12$). (B and D) Time course of MgT effect on spatial working memory of young and aged rats. Data are calculated as the difference in correct choices between control (n = 12) and MgT-treated (n = 12) rats. One-way ANOVA analysis revealed significant differences (compared with day 0) as follows: young rats $F_{10,121} = 7.08$, $p < 0.0001$; aged rats $F_{12,143} = 16.38$, $p < 0.0001$). Bonferroni's post hoc test, *p < 0.05, ***p < 0.001. Data are presented as mean ± SEM. See also Figure S5.

$p < 0.001$, Figure 1A). Other magnesium compounds did not elevate $[Mg^{2+}]_{CSF}$ significantly when compared to control (Figure 1A).

We further verified that the compound with high bioavailability and loading ability into brain is the best Mg^{2+} compound for studying the effects of elevating brain Mg^{2+} on memory. For this propose, we determined the effective dose for memory enhancement first.

Control rats were fed ordinary rat chow containing 0.15% Mg^{2+} (see Experimental Procedures), which is considered standard. Different MgT doses were given to rats and their performances on learning behavior in the water maze task were compared. We found that 50 mg/kg/day (elemental Mg^{2+}) is the minimum effective dose (see Figure S2A). In a separate memory test, the novel object recognition test (NORT), when the actual dose consumed by individual rats varied due to the difference in daily fluid intake, the effective dose was still around 50 mg/kg/day (see Figure S2B). Therefore, 50 mg/kg/day was used in this study. Chronic (1 month) MgT treatment at this dose did not influence water and food intake, body weight, and overall mobility (see Figure S3).

Next, rats were treated with various magnesium compounds for 1 month via drinking water at a dose of 50 mg/kg/day elemental Mg^{2+}. We used aging rats (18 month) because they already have memory decline (compared to younger rats) in order to increase the possibility of observing memory improvement. Rats treated with MgT showed significant enhancement of short-term memory (10 min retention interval, one-way ANOVA analysis, $p < 0.05$) using a modified NORT (see Figure S4 and Supplemental Experimental Procedures). Rats treated with magnesium-chloride or -citrate displayed enhanced short-term memory as well, but this enhancement was not statistically significant (Figure 1B). Surprisingly, although magnesium-gluconate in milk has a comparable bioavailability to MgT (X.Z., F. Mao, Y. Shang, N.A., and G.L., unpublished data), it failed to enhance memory (Figure 1B). For the long-term memory test (12 hr retention interval), only MgT-treated rats exhibited enhanced performance ($p < 0.05$, Figure 1C). To test whether threonate per se has any positive effect on memory, we assessed the effect of sodium-L-threonate on memory; no effect was observed (Figures 1D and 1E). We also examined the effectiveness of the combination of magnesium-chloride with sodium-L-threonate, as the mixture of both forms the MgT complex in aqueous solution. To our surprise, this combination was ineffective (Figures 1D and 1E). Hence, we chose MgT as the optimal testing compound to study the effects of elevating brain Mg^{2+} on memory and its underlying molecular and cellular mechanisms.

Enhancement of Spatial Working Memory by MgT

We tested rats for several hippocampus-dependent forms of memory. Spatial working memory was assessed using a T-maze non-matching-to-place task (Dudchenko, 2001). Naive untreated rats were trained for 10 days on a reward forced-choice alternation task (see Supplemental Experimental Procedures). The percentage of correct choices (alternations) was recorded for each daily session. Following 8 days of training, all rats attained an asymptotic choice accuracy level of ~94%, indicating that they learned the task. In these experiments, the rats likely used a spatial strategy because when the maze was rotated by 180°, the rats went to the arm predicted by allocentric, rather than egocentric, coordinates (data not shown).

At the end of the training, rats were assigned to control and MgT-treated groups to assure each group had a comparable average working memory capability. Spatial working memory was tested by a gradual increase of the delay between sample and choice trials, before (day 0) and after (day 24) MgT treatment (Figures 2A and 2C). The choice accuracy of control young rats did not change significantly (see Figure S5A). On the other hand, MgT-treated young rats had significantly better performance than untreated rats at the longest delay interval (5 min, $p < 0.05$, Figures 2A). For control aged rats, their choice accuracy declined slightly during the experimental period (see Figure S5B). However, MgT-treated aged rats displayed significantly better performance than untreated aged rats in 5 min delay interval ($p < 0.05$, Figure 2C). Thus, MgT treatment can enhance spatial working memory in young and aged rats. Spatial working memory evaluated by T-maze did not significantly decline with aging under our experimental conditions. However, aged rats learned the alternating T-maze task slower than young rats and MgT treatment in aged rats prevented such deficit (data not shown).

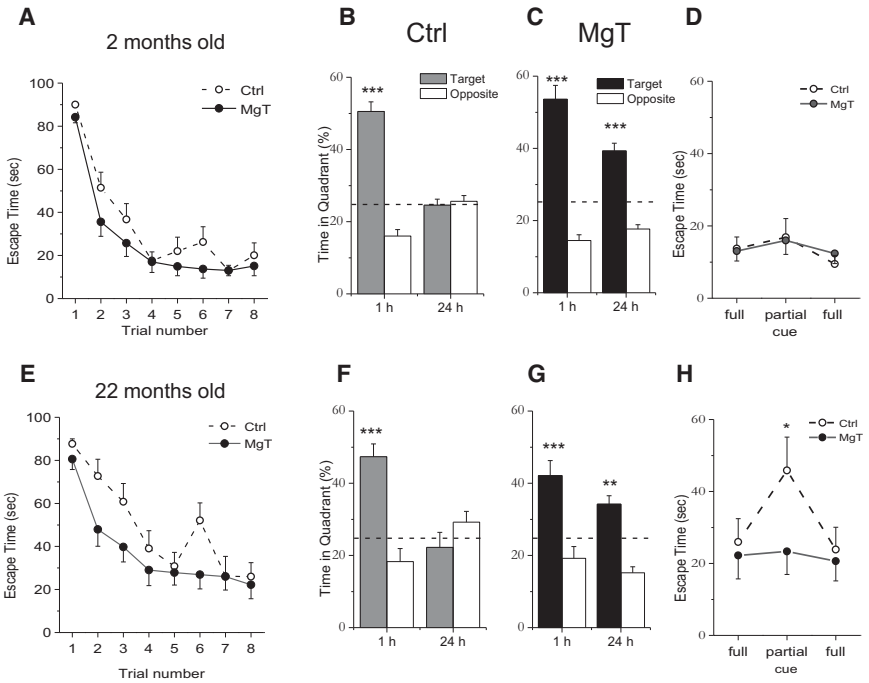

Figure 3. Enhancement of Spatial Long-Term Memory in Water Maze by MgT

(A) Escape time to find the hidden platform of young rats during the water maze training trials. MgT-treated (n = 15) rats learned faster than controls (n = 14, two-way ANOVA, $F_{1,216} = 7.85$, $p = 0.006$). ANOVA was followed by Bonferroni's post hoc test.

(B and C) Percentage of time spent in the target versus opposite quadrant during the first (1 hr after training) and the second (24 hr after training) probe trials in control (n = 14, B) and MgT-treated (n = 15, C) young rats. During the first probe trial, both groups spent significantly more time in the target quadrant (paired t test, $p < 0.0001$). On the other hand, only MgT-treated rats spent significantly more time in the target quadrant during the second test trial (24 hr after training, $p < 0.0001$).

(D) Pattern completion test with partial extra maze cues of young rats. Partial cues did not impair the rats' ability to find the platform.

(E) Escape time of aged rats. MgT-treated (n = 12) rats learned faster than controls (n = 16, ANOVA, $F_{1,208} = 11.42$, $p = 0.0009$).

(F and G) Performance of control (n = 16, F) and MgT-treated (n = 12, G) aged rats during the first (1 hr after training) and the second (24 hr after training) memory probe trials. During the first trial, both groups spent more time in the target quadrant (paired t test, $p < 0.0001$). Twenty-four hours later, only MgT-treated aged rats spent more time in the target quadrant ($p < 0.01$).

(H) Partial removal of extra-maze cues impaired the ability of aged rats to find the hidden platform, while MgT-treated aged rats were still capable of locating the platform (unpaired t test, $p < 0.05$). *$p < 0.05$, **$p < 0.01$, ***$p < 0.001$. Data are presented as mean ± SEM. See also Table S1.

To monitor the time-course of MgT treatment on working spatial memory, task performance was evaluated every sixth day (Figures 2B and 2D). Since the largest difference in choice accuracy between the treated versus control rats was obtained at 5 min delay interval, we monitored choice accuracy only at this delay interval for the remaining experiments. A significant increase in choice accuracy of MgT-treated young rats was apparent 6 days after the onset of treatment (one-way ANOVA, $p < 0.05$), peaked on day 12 ($p < 0.001$), and did not decline over 1 month after MgT treatment was stopped (days 30 to 60, Figure 2B). For MgT-treated aged rats, a significant increase in choice accuracy occurred 12 days after the onset of treatment ($p < 0.001$) and remained stable until MgT was stopped (day 30). In contrast to young rats, the working memory performance of aged rats declined to the baseline value within 12 days following interruption of MgT treatment (Figure 2D). Therefore, the on/off kinetics of MgT-induced spatial memory enhancement seems symmetric in aged rats. To test if MgT could re-enhance spatial memory functions of MgT-treated aged rats, following 30 days of drinking plain water (days 30–60), they drank water supplemented with MgT again. Strikingly, aged rat performance was re-enhanced within 12 days of treatment (Figure 2D). Thus, MgT consumption enhanced spatial working memory of young and aged rats (For the detailed time course curves for each group, see Figures S5C and S5D).

Enhancement of Spatial Long-Term Memory by MgT

We used the Morris water maze to perform further experiments to determine whether MgT leads to the improvement of spatial long-term memory (Morris, 1984). Young rats underwent 8 trials of training within one day with a 1 hr intertrial interval. For aged rats, the training protocol was spread over two days: 5 trials on day 1, and 3 trials on day 2. This protocol was adopted because aged rats are not able to perform 8 trials within one day. During the training period, the performance of all rats gradually improved (Figures 3A and 3E). However, MgT-treated rats learned to find the hidden platform faster than controls (two-way ANOVA, MgT-treated versus control young rats, $p < 0.01$ and MgT-treated versus control aged rats, $p < 0.001$). In addition, the degree of learning ability enhancement by MgT was higher in aged (Figure 3E) than in young rats (Figure 3A).

To evaluate memory functions, we performed two test trials with the platform removed; the rats were allowed to search for 60 s. The first test trial commenced 1 hr after the end of training. All rats showed a remarkable preference for the target versus opposite quadrant (young, Figures 3B and 3C, paired t test, $p < 0.001$; old, Figures 3F and 3G, $p < 0.001$), suggesting that all, i.e., control and MgT-treated young and aged rats, could remember the platform location. To test long-term spatial memory, a second test trial was performed 24 hr later. Both young and aged control rats lost their preference for the target quadrant compared to other quadrants (Figures 3B and 3F). In contrast, MgT-treated young (Figure 3B) and aged (Figure 3G) rats retained their quadrant preference ($p < 0.001$; $p < 0.01$, respectively). Visual and locomotor functions were equal in both groups, as judged by latency of escape to a visible platform (data not shown) and swimming speed (see Table S1). Thus,

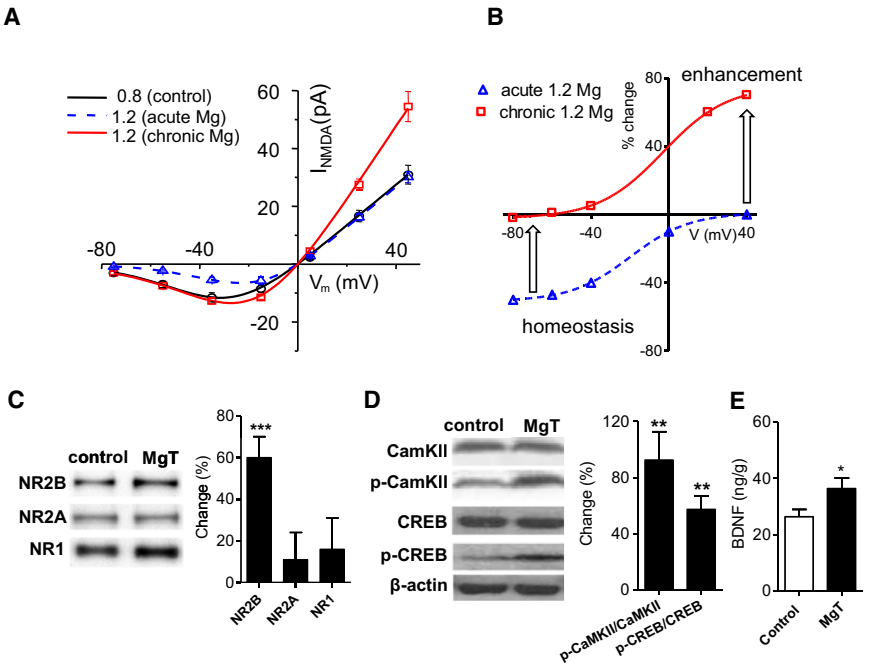

Figure 4. The Effects of Mg^{2+} on NMDAR Activation, Expression, and Its Downstream Signaling Molecules

(A) Voltage dependency of I_{NMDA} evoked by glutamate iontophoresis at putative synapses in 0.8 Mg^{2+} cultures (black line, n = 7), following acute (<1 hr, blue dashed line, n = 7) and chronic (red line, n = 7) elevation of $[Mg^{2+}]_o$ to 1.2 mM.

(B) Percent change of I_{NMDA} following acute (blue dashed line) and chronic (red line) elevation of $[Mg^{2+}]_o$.

(C) Quantitative analysis of expression of NMDAR subunits using western blots in the hippocampus of control and MgT-treated rats. MgT significantly increased NR2B subunit ($p < 0.0001$, n = 8), without altering NR2A and NR1 subunits.

(D) Same as (C), but of expression/phosphorylation of NMDAR downstream signaling molecules. MgT significantly increased phosphorylation of CamKII ($p < 0.01$, n = 7) and CREB ($p < 0.01$, n = 8) without altering the expression level of both proteins. Data are presented as percentage of change relative to control. β-actin was used as loading control.

(E) Quantitative analysis of BDNF protein level in the hippocampus using ELISA kit. MgT significantly increased BDNF expression ($p < 0.05$, n = 10). Unpaired t test, *$p < 0.05$, **$p < 0.01$, ***$p < 0.001$. Data are presented as mean ± SEM.

MgT treatment significantly enhanced hippocampus-dependent spatial learning and memory in both young and aged rats.

Improvement of Memory Recall by MgT

A crucial cognitive function requiring memory is pattern completion, i.e., the ability to retrieve memories based on incomplete information, a capability that declines profoundly during aging (Gallagher and Rapp, 1997). To test this capability, we compared the dependence of spatial memory recall on the integrity of extra-maze cues in young and aged control and MgT-treated (for 1 month) rats following the water maze training period. For control aged rats, the integrity of the extra-maze cues from surrounding curtains was essential for finding the hidden platform, as their performance significantly degraded under partial-cue conditions. In contrast, MgT-treated aged rats, as well as young rats, performed equally well under full- and partial-cue conditions (aged rats, Figure 3H, unpaired t test, $p < 0.05$; young rats, Figure 3D). Thus, MgT treatment enhanced memory recall under partial information conditions in aged but had no effect on young, rats.

Enhancement of NMDAR-Dependent Signaling by MgT

The above data indicate that elevating brain Mg has positive influence on learning and memory function. We have performed the following experiments to explore the possible molecular mechanisms underlying this memory enhancement. We focused on NMDAR-dependent signaling because its activation is critical for synaptic plasticity and memory (for review, see Martin et al., 2000; Nakazawa et al., 2004) and increase in NMDAR in synapses can enhance learning and memory (Lee and Silva, 2009). Mg^{2+}, an important regulator of NMDAR channel opening (Mayer et al., 1984; Nowak et al., 1984), can have strong influence on NMDAR-dependent signaling. Thus, enhancement of learning and memory with elevating brain Mg^{2+} might be at least, in part, caused by alteration of NMDAR-dependent signaling. However, as NMDAR channel opening can be blocked by $[Mg^{2+}]_o$, increase in brain Mg^{2+} would increase NMDAR channel blockage, which might lead to downregulation of NMDAR-dependent signaling, resulting in impairment of learning and memory.

To address these issues, we studied the NMDAR currents under different $[Mg^{2+}]_o$. Using iontophoretic application of glutamate to a putative postsynaptic site exactly as described before (Murnick et al., 2002), we isolated the postsynaptic I_{NMDA} for biophysical studies in vitro. Figure 4A shows the average I_{NMDA} from synapses grown under 0.8 mM $[Mg^{2+}]_o$ (black line, n = 7 cells). When $[Mg^{2+}]_o$ was elevated to 1.2 mM acutely, amplitude of I_{NMDA} near resting membrane potential was reduced by ~50%, suggesting that the amplitude of I_{NMDA} near resting membrane potential is very sensitive to small increase in $[Mg^{2+}]_o$. On the other hand, the size of I_{NMDA} under positive membrane potentials remained the same (blue dashed line, n = 7 cells). Thus, at higher $[Mg^{2+}]_o$, strong depolarization is still capable of expelling Mg^{2+} from mouth of NMDAR and removing Mg^{2+} block completely. Interestingly, when $[Mg^{2+}]_o$ were elevated chronically (cultures were grown and recorded under 1.2 mM $[Mg^{2+}]_o$, red line, n = 7 cells), the amplitudes of the I_{NMDA} recorded near resting membrane potential were almost identical with I_{NMDA} from synapses grown under 0.8 mM $[Mg^{2+}]_o$, while the amplitudes of I_{NMDA} at positive membrane potentials were significantly larger. This phenomenon can be visualized more directly in Figure 4B, where the percentage of I_{NMDA} changes in acute versus chronic elevation of $[Mg^{2+}]_o$ is plotted as a function of membrane potential. These data suggest that reduction in I_{NMDA}

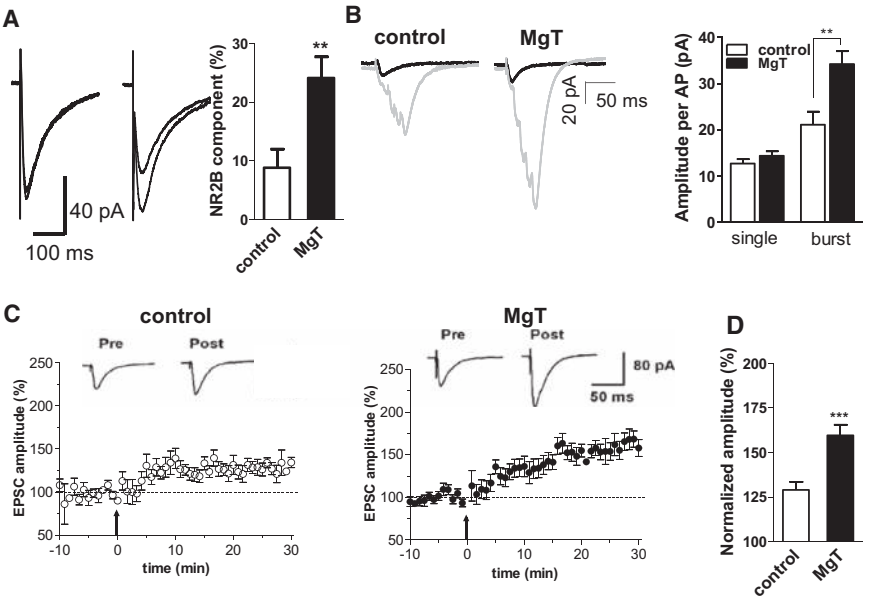

Figure 5. Enhancements of Synaptic Facilitation and Long-Term Potentiation by MgT

(A) Representative averaged (30 sweeps) traces of $EPSC_{NMDA}$ with/without blocking of the NR2B-containing NMDAR by ifenprodil (3 μM). In controls (n = 5), the $EPSC_{NMDA}$ amplitude slightly reduced by ifenprodil, while in MgT-treated rats (n = 5), the reduction of amplitude was significantly higher ($p < 0.01$, right panel).

(B) Representative averaged (30 sweeps) traces of $EPSC_{AMPA}$ (−70 mV, 50 μM AP-5) evoked by two patterns of stimulation: single APs (black line, 0.1 Hz) and bursts (gray line, each burst contains 5 APs, ISI = 10 ms, interburst interval 10 s) in control and MgT-treated rats. Right panel: averaged $EPSC_{AMPA}$ amplitudes of control (n = 6) and MgT-treated (n = 7) rats. The averaged amplitude of $EPSC_{AMPA}$ per AP for bursts was significantly higher in MgT-treated rats ($p < 0.01$).

(C) Long-term potentiation induced in pyramidal neurons in hippocampal slices of control rats (n = 10, left panel) by the pairing training protocol (indicated by an arrow). The insets show averages of six $EPSC_{AMPAs}$ 5 min before and 30 min after LTP induction. The dashed line indicates the mean basal synaptic responses. Right panel: LTP induced in hippocampal slices of MgT-treated rats (n = 12).

(D) The magnitude of long-term potentiation (average over last 5 min) following "pairing training" was significantly higher in MgT-treated group ($p < 0.001$). Unpaired t test, $^{**}p < 0.01$, $^{***}p < 0.001$. Data are presented as mean ± SEM.

near resting membrane potential triggers a compensatory upregulation of postsynaptic NMDAR (Slutsky et al., 2004), which restores I_{NMDA} to its original level (Figures 4A and 4B, red line). However, the removal of the Mg^{2+} block during strong depolarization (correlated inputs) exposes these additional NMDAR, resulting in a selective increase in NMDAR activity during strong depolarization (Figures 4A and 4B, red line). Therefore, the ultimate effects of elevating $[Mg^{2+}]_o$ would be the upregulation of NMDAR and the enhancement of NMDAR-dependent signaling associated with correlated synaptic activity.

We checked these predictions in rats treated with MgT. First, the expression levels of NMDAR subunits in control and MgT-treated rats were compared. Chronic MgT treatment selectively increased the expression of NR2B subunit (~60% of control, t test, $p < 0.001$) in hippocampus homogenate, while the expression of other subunits of NMDAR (NR2A and NR1) was unchanged (Figure 4C). These data are consistent with our previous observations that increase in $[Mg^{2+}]_o$ can trigger upregulation of NR2B-containing NMDAR (Slutsky et al., 2004). Next, we assessed whether the upregulation of NR2B-containing NMDAR leads to increase in activation of NMDAR-dependent signaling by examining the activation of α-CaMKII and CREB following NORT memory task (described above). After LTM test (24 hr retention interval), rats were decapitated and hippocampi were dissected. MgT treatment did not change the expression level of CaMKII and CREB but increased their activation. As a result, the ratio of phosphorylated-CaMKII/total CaMKII was increased (92%, $p < 0.01$), as was the ratio of phosphorylated-CREB/total CREB (57%, $p < 0.01$, Figure 4D). Therefore, NMDAR-dependent signaling is enhanced in MgT-treated rats. To further confirm the beneficial effects of increase in NMDAR signaling, we quantified the expression level of the neurotrophic factor BDNF, a protein regulated by level of CREB activation. BDNF protein expression was significantly higher in MgT-treated rats (36%, $p < 0.05$, Figure 4E).

Enhancement of Synaptic Plasticity by MgT

To test the effects of enhancing NMDAR signaling on synaptic plasticity, we compared synaptic transmission and plasticity in control and MgT-treated rats. First, we determined if the increase in NR2B subunit expression was associated with changes in NMDAR-mediated synaptic transmission, and we recorded the $EPSC_{NMDA}$ between CA3-CA1 synaptic connections (Shaffer collaterals) in hippocampal slices using whole-cell patch-clamp recordings (V_{hold} = −50 mV) in visually identified CA1 pyramidal neurons while stimulating Shaffer collaterals at low frequency (0.03 Hz). We measured the sensitivity of $EPSC_{NMDA}$ to ifenprodil, a selective antagonist of NR2B subunits (Williams, 1993). Similar to our results in cultured hippocampal synapses (Slutsky et al., 2004), the sensitivity of $EPSC_{NMDA}$ to ifenprodil (3 μM) significantly increased from 8.8 ± 3.1% to 24.1 ± 3.6% in slices from MgT-treated rats (n = 5 cells, $p < 0.01$, Figure 5A). Therefore, the detected increase of NR2B expression is associated with an increase in the ratio of NR2B/NR2A in synapses.

Next, we tested whether MgT treatment affects synaptic facilitation of hippocampal excitatory synapses. The input-output relationship in CA3-CA1 synaptic connections in hippocampal slices of control and MgT-treated aging rats was evaluated. Two types of input patterns—single action potentials (APs) and bursts (each burst contained 5 APs, ISI = 10 ms)—were applied through minimal stimulation of Shaffer collateral axons. Output was measured by whole-cell patch-clamp recordings in pyramidal CA1 neurons of AMPA-mediated excitatory postsynaptic

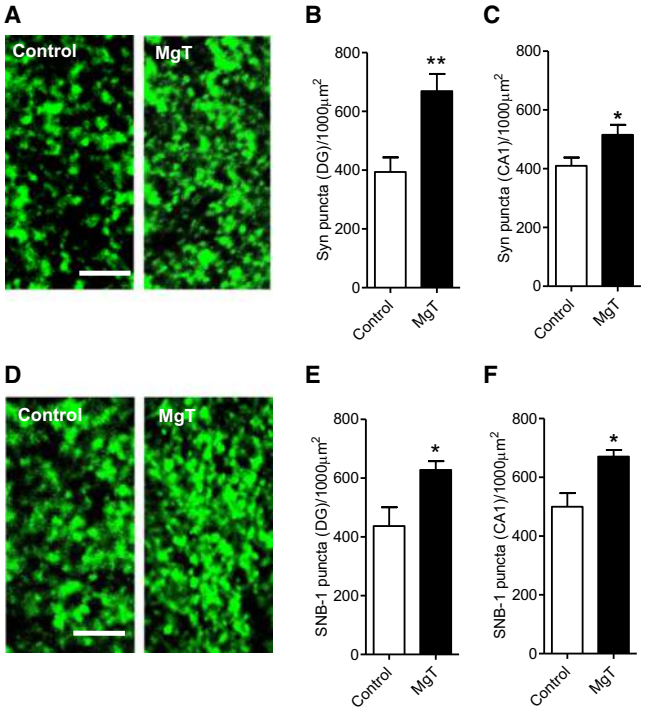

Figure 6. Increase in Density of Syn- and SNB-1-Positive Puncta in MgT-Treated Aged Rats

(A) Synaptophysin (Syn)-immunostained puncta in control and MgT-treated aged rats (22 months old).

(B and C) The density of Syn-(+) puncta in the DG and CA1 of control (n = 10) and MgT-treated (n = 6) aged rats. MgT treatment increased the number of Syn-(+) puncta in the DG (B, $p < 0.01$) and CA1 (C, $p < 0.05$).

(D) Synaptobrevin (SNB1)-immunostained puncta in the same control and MgT-treated aged rats.

(E and F) MgT treatment increased the density of SNB1-(+) puncta in the DG (E, $p < 0.05$) and CA1 (F, $p < 0.05$). The density was estimated as the number of immunostained puncta per 1000 μm^2. Scale bar, 10 μm. Unpaired t test, *$p < 0.05$, **$p < 0.01$.

current ($EPSC_{AMPA}$). MgT treatment did not affect $EPSC_{AMPA}$ amplitude for single APs but significantly enhanced $EPSC_{AMPA}$ amplitude for bursts (control: n = 6 cells; MgT: n = 7 cells, $p < 0.01$, Figure 5B).

Long-term changes in synaptic strength are hypothesized to form the cellular basis of information storage and memory (Martin et al., 2000). A synapse with increased amounts of NR2B-containing NMDAR (Tang et al., 1999) and strong synaptic facilitation (Bi and Poo, 1998) is expected to have higher magnitude of LTP. $EPSC_{AMPA}$ in CA1 neurons was recorded while stimulating Shaffer collaterals at low frequency (0.03 Hz). After stable recording was achieved (10 min), a spike-timing-dependent plasticity induction protocol (Bi and Poo, 1998; Markram et al., 1997) was applied. This protocol produced a persistent LTP in slices from both control and MgT-treated aged rats (control: n = 10 cells, $p < 0.001$ versus baseline responses before the pairing training; MgT: n = 12 cells, $p < 0.01$, Figure 5C). However, the magnitude of LTP in slices from MgT-treated rats was higher than controls (~52%, $p < 0.0001$, Figure 5D). In slices that were not subjected to the pairing protocol, synaptic responses were not significantly altered over the entire recording period (last 5 min mean = 93.5 ± 8.9% of first 5 min baseline response, n = 5 cells).

Therefore, synapses in MgT-treated rats exhibited higher activation/expression of plasticity/memory-related proteins and enhancement of both short-term and long-term synaptic potentiation.

MgT Increased the Density of Synaptophysin-Positive Puncta

Several studies indicate that synaptic connections in hippocampus decline during aging, with the degree of loss of synapses correlating with the impairment of memory functions (Burke and Barnes, 2006; Geinisman et al., 2004; Smith et al., 2000; Wilson et al., 2006). The reduction seems to be hippocampal subregional specific. For example, the stratum moleculare of the dentate gyrus (DG) is the most vulnerable brain region for age-related synaptic loss (Burke and Barnes, 2006; Geinisman et al., 2004; Smith et al., 2000; Wilson et al., 2006). The loss of synaptic connections in the stratum radiatum of CA1 subregion is less than DG and remains controversial (Burke and Barnes, 2006; Geinisman et al., 2004).

To further characterize the potential cellular mechanisms that underlie MgT-induced memory enhancement, we investigated the effect of 1 month of MgT treatment on density of presynaptic boutons in aged rats (22 months). Rats were anesthetized and perfused, and the number of synaptophysin-positive (Syn-[+]) puncta in the stratum moleculare was measured. Figure 6A shows Syn-(+) puncta in the DG of hippocampus. Indeed, the density of Syn-(+) puncta in MgT-treated rats was significantly higher than controls (~67%, t test, $p < 0.01$, Figure 6B). We also estimated the density of Syn-(+) puncta in CA1 and found that it was ~25% higher in MgT-treated aged rats than aged controls ($p < 0.05$, Figure 6C). A similar pattern of changes was observed with another presynaptic protein synaptobrevin (SNB1) (Figure 6D). MgT increased density of SNB1-(+) puncta by ~43% in the DG and ~34% in the CA1 subregions of hippocampus ($p < 0.05$, Figures 6E and 6F). The density of Syn-(+) and SNB1-(+) puncta have been correlated per individual rat (Pearson test, $r^2 = 0.58$, $p = 0.0006$, Figure S6A). Thus, MgT treatment increased the density of presynaptic boutons containing vesicle proteins critical for transmitter release in DG and CA1 of aged rats.

It is worth noting that presynaptic boutons with very low concentration of synaptophysin/synaptobrevin will not be counted by our present approach, therefore, we might have underestimated the actual density of presynaptic Syn-/SNB1-(+) boutons. Since synaptobrevin is essential for synaptic vesicle fusion (Schiavo et al., 1992), a presynaptic bouton with low synaptobrevin concentration may not be functional. Under these considerations, increase in the density of Syn- and/or SNB1-(+) puncta could be due to increase in either density of presynaptic boutons or amount of these proteins in the existing boutons.

Increased Functional Synaptic Connection by Elevated $[Mg^{2+}]_o$

Does Mg^{2+}-induced increase in Syn- / SNB1-(+) puncta lead to increase in the number of functional release sites, and,

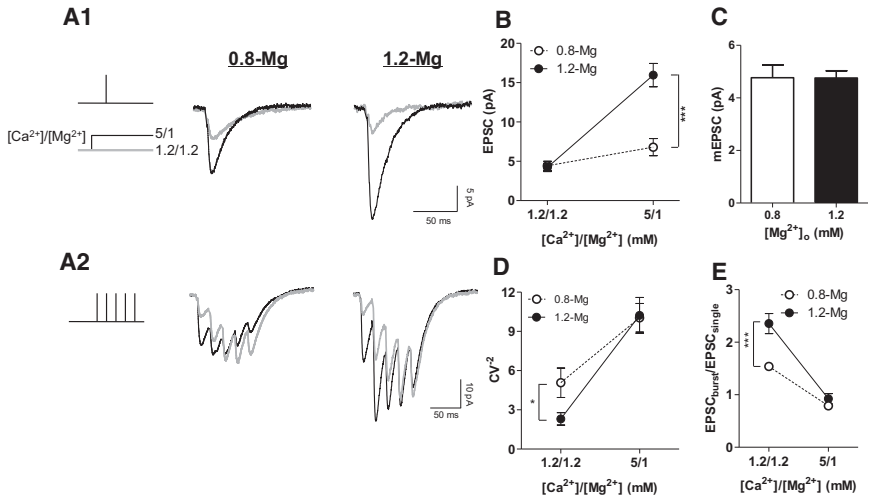

Figure 7. Increase in Presynaptic Release Sites and Decrease in Pr of Synapses by Elevation of $[Mg^{2+}]_o$

(A_1 and A_2) Mean $EPSC_{AMPA}$ recorded at −70 mV (average of 30 sweeps) and evoked by minimal stimulation at low frequency (upper traces, 0.1 Hz) and by bursting input (bottom traces; bursts of 5 APs, ISI = 20 ms, interburst interval 0.1 Hz) under low (1.2 mM, gray trace) and high (5 mM, black) $[Ca^{2+}]_o$ in 0.8 and 1.2 Mg slices.

(B) Mean $EPSC_{AMPA}$ under low and high $[Ca^{2+}]_o$ (n = 10). The $EPSC_{AMPA}$ was similar under physiological $[Ca^{2+}]_o$, but significantly higher ($p < 0.0001$) in 1.2-Mg slices under high $[Ca^{2+}]_o$.

(C) The quantal size in 0.8 and 1.2 Mg slices was similar (n = 10).

(D) CV^{-2}, calculated as variance^2/mean^2, was significantly higher ($p < 0.05$, n = 10) in 1.2 Mg slices at physiological $[Ca^{2+}]_o$ but similar at high $[Ca^{2+}]_o$.

(E) Synaptic facilitation, defined by the ratio of $EPSC_{burst}/EPSC_{single}$, was higher in 1.2-Mg slices at physiological $[Ca^{2+}]_o$ (n = 10, $p < 0.001$), but similar under high $[Ca^{2+}]_o$. $EPSC_{single}$ is the amplitude of $EPSC_{AMPA}$ for single AP input, and $EPSC_{burst}$ is the mean amplitude of $EPSC_{AMPA}$ per single AP within the burst. Unpaired t test, *$p < 0.05$, ***$p < 0.001$. Data are presented as mean ± SEM.

subsequently, enhance synaptic transmission? To address this question, we studied the properties of synaptic transmission in hippocampal slices treated with different $[Mg^{2+}]_o$.

In cultured hippocampal neurons, plasticity (Slutsky et al., 2004) and density (I.S., H. Zhou, and G.L., unpublished data) of functional presynaptic boutons increased 4 hr following elevation of $[Mg^{2+}]_o$ from 0.8 mM to 1.2 mM. Therefore, freshly cut hippocampal slices (from 2-month-old rats) were incubated for 5 hr in ACSF containing different $[Mg^{2+}]_o$ (0.8 and 1.2 mM, referred to as 0.8 and 1.2 Mg slices). Irrespective of incubation conditions, the baseline recording solution contained constant, 1.2 mM, $[Mg^{2+}]_o$ before switching to test solutions. Whole-cell patch-clamp recordings were made on pyramidal CA1 neurons, and $EPSC_{AMPA}$s were evoked by minimal stimulation of Shaffer collateral axons in the presence of an NMDAR blocker (50 μM AP-5).

According to Katz's quantal hypothesis, the efficacy of a synaptic connection is determined by the product of the probability of release (Pr), the number of release sites ($n_{release}$), and the size of the postsynaptic response to a quantum of transmitter (q) (Katz, 1969). Although the number of release sites can be estimated using the conventional quantal analysis, this approach requires a good voltage clamp of dendritic synapses, which is difficult to obtain for neurons in CNS (Williams and Mitchell, 2008). Since presynaptic release is very sensitive to Ca^{2+}, even without adequate voltage clamp, any difference in EPSC amplitudes under various $[Ca^{2+}]_o$ is most likely due to difference in Pr and/or $n_{release}$ (Clements, 2003; Silver, 2003). Therefore, we inferred the number of functional release sites by studying synaptic transmission under various $[Ca^{2+}]_o$. Figure 7A_1 shows recordings of the evoked $EPSC_{AMPA}$ for a single AP under various $[Ca^{2+}]_o$ in 0.8 Mg versus 1.2 Mg slices. The amplitudes of $EPSC_{AMPA}$ were almost identical under physiological concentrations of Ca^{2+} (1.2 mM; Figure 7A_1 gray, and Figure 7B), suggesting that incubation of slices under higher $[Mg^{2+}]_o$ did not influence basal synaptic strength. When $[Ca^{2+}]_o$ was elevated in test recording solution to 5 mM in order to maximize the Pr, $EPSC_{AMPA}$ amplitudes in both slices increased correspondingly; however, the degree of increase was 2.4-fold higher in 1.2 Mg than 0.8 Mg slices (n = 10 cells, t test, $p < 0.0001$, Figure 7A_1 black and Figure 7B). There was no difference in quantal size between 0.8 Mg and 1.2 Mg slices (n = 10 cells, Figure 7C). Therefore, the increase in $EPSC_{AMPA}$ amplitudes at higher $[Ca^{2+}]_o$ in 1.2 Mg slices is likely due to higher number of functional release sites per axon.

Notably, $EPSC_{AMPA}$ amplitude was the same under physiological $[Ca^{2+}]_o$ (1.2 mM, Figure 7B) in both groups of slices, meaning that $Pr \times n_{release} \times q_{(0.8\text{-}Mg)} = Pr \times n_{release} \times q_{(1.2\text{-}Mg)}$. Thus, the Pr of synaptic boutons in 1.2 Mg slices must be lower to counterbalance the increase in the number of release sites per connection. To test this possibility, the $EPSC_{AMPA}$ coefficient of variation was used to estimate the Pr ($Pr \sim CV^{-2}$, [Clements, 2003; Malinow and Tsien, 1990; Silver, 2003]). CV^{-2} was 2.0-fold lower in 1.2 Mg slices (n = 10 cells, $p < 0.05$, Figure 7D), suggesting that these synapses do have lower Pr under physiological $[Ca^{2+}]_o$. Application of the coefficient of variation to determine the quantal parameters involves several assumptions, such as nearly all variances are presynaptic, which cannot be verified directly (Clements, 2003). We applied another independent method to estimate Pr of synapses by calculating the degree of short-term facilitation, which primarily depends on presynaptic factors. Low Pr synapses tend to have higher facilitation index (Zucker and Regehr, 2002). Indeed, the synaptic facilitation of 1.2 Mg slices during bursts was 2.3-fold higher than that of 0.8 Mg slices (n = 10 cells, $p < 0.001$, Figures 7A_2 and 7E). Therefore, Pr of synaptic boutons is likely to be lower in 1.2 Mg than in 0.8 Mg slices. To further verify the validity of both methods, we compared CV^{-2} and the facilitation in 0.8 Mg and 1.2 Mg slices under high $[Ca^{2+}]_o$. Pr of synapses under high $[Ca^{2+}]_o$ is expected to be maximized. Under this condition, the differences in CV^{-2} and the facilitation between 0.8 and 1.2 Mg slices should disappear. Consistent with this prediction, CV^{-2} and facilitation were

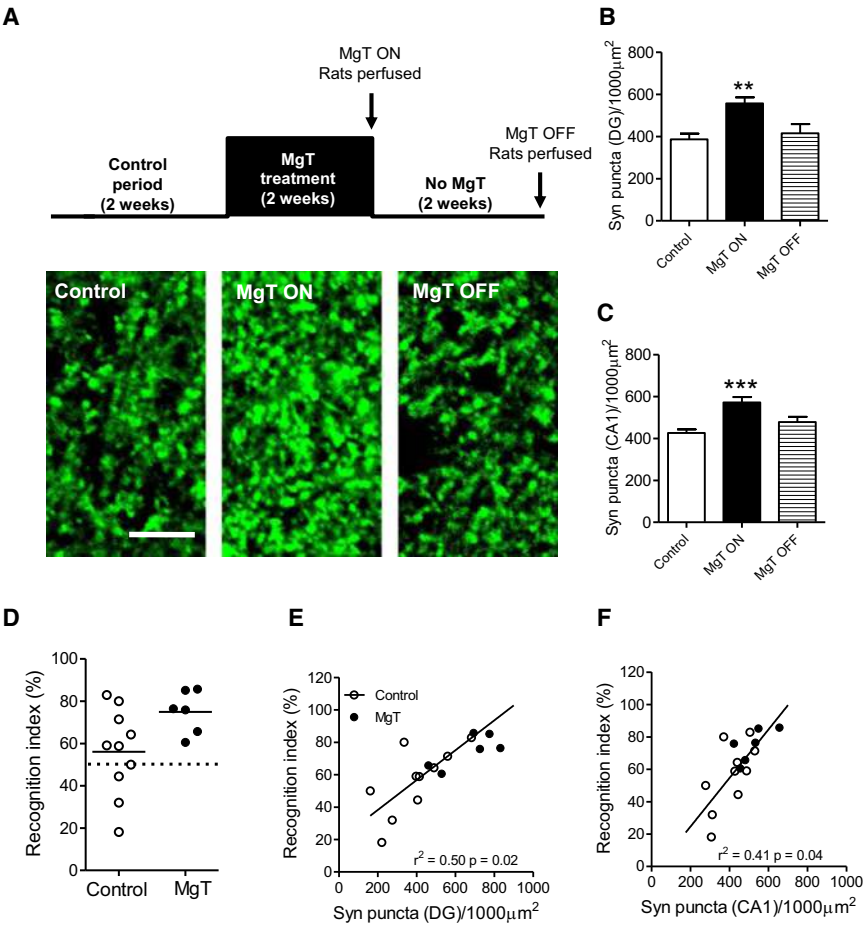

Figure 8. Correlation among MgT Treatment, Synaptic Bouton Density, and Memory

(A) Temporal relationship between "on/off" of MgT treatment and the density of Syn-(+) puncta. Syn-(+) puncta increased 2 weeks after MgT treatment (MgT ON) and returned to control level 2 weeks after stopping MgT treatment (MgT OFF). Scale bar, 10 μm.

(B and C) Quantitative analysis of the density of Syn-(+) puncta in DG and CA1 of control (n = 10), MgT ON (n = 5) and MgT OFF (n = 5) rats (one-way ANOVA, DG, $F_{2,17}$ = 6.88, p = 0.0065; in CA1, $F_{2,17}$ = 11.45, p = 0.0007). ANOVA was followed by Bonferroni's post hoc test (**p < 0.01; ***p < 0.0001).

(D) The short-term memory varied among individual aged rats as revealed by the recognition index of novel object recognition test. Rats treated with MgT spent more time exploring the novel object (n = 6) than controls (n = 10).

(E) The density of Syn-(+) puncta in the DG correlated with the recognition index of individual control rats. MgT-treated rats' data were not included in the correlation analysis, although data are displayed on the figure. No significant correlation was found in MgT-treated group.

(F) The density of Syn-(+) puncta in the CA1 also correlated with the recognition index of individual control rats (Pearson test). MgT-treated rats' data were not included in the correlation analysis. Data are presented as mean ± SEM. See also Figure S6.

the same between both groups of slices under high $[Ca^{2+}]_o$ (5 mM, Figures 7D and 7E).

Therefore, elevation of $[Mg^{2+}]_o$ can trigger increase in the number of functional presynaptic release sites with lower release probability. This synaptic reconfiguration maintains homeostasis of AMPA-mediated synaptic transmission for a single AP (Figures 7A and 7B) yet enhances transmission for bursting inputs (Figure 7E), similar to the observations in slices from MgT-treated rats (Figure 5B).

Correlation between Density of Synaptophysin-Positive Presynaptic Boutons and Memory

The above data demonstrate that increase in brain Mg^{2+} leads to increase in functional connectivity, synaptic plasticity, and enhancement of learning and memory. To further assess the impact of increase in density of presynaptic boutons to memory enhancement, we performed the following two sets of experiments.

In the T-maze task, memory performance reached maximum 12 days after the onset of MgT treatment and dropped to baseline 12 days after the offset of MgT treatment in aged rats. If a change in the density of Syn-(+) puncta contributes to memory enhancement, both parameters are expected to change correspondingly. Indeed, when aged rats (22 month) were treated with MgT for 2 weeks, the density of Syn-(+) puncta increased in DG (~44%, one-way ANOVA, p < 0.01, Figures 8A and 8B) and in CA1 (~30%, p < 0.0001, Figure 8C) hippocampal areas. On the other hand, the density of Syn-(+) puncta in MgT-treated rats (2 weeks of treatment) returned to the control level 2 weeks after the end of MgT supplementation (Figures 8A, 8B, and 8C). Thus, the time course of change in the density of Syn-(+) puncta following on/off MgT treatment matched the time course of alterations in memory score.

Next, we studied whether the density of Syn-(+) puncta is correlated to the memory score per individual rat. The short-term memory of aged rats (different from those used for T-maze experiments) was evaluated using the novel object recognition test with two objects. After behavioral assessment, rats were sacrificed and analyzed for Syn- / SNB1-(+) puncta density. The short-term memory among untreated aged rats varied significantly as revealed by their recognition index (Figure 8D), a phenomenon that had been reported previously (Gallagher and Rapp, 1997; Smith et al., 2000). MgT treatment enhanced memory and reduced the individual variation among treated aged rats (Figure 8D). Interestingly, the density of Syn-(+) puncta in DG correlated with the recognition index per individual rat of control group (Figure 8E, Pearson test, r^2 = 0.50, p = 0.02). The density of Syn-(+) puncta in CA1 of control group also correlated with recognition index, though the correlation was slightly weaker than in DG (Figure 7F, r^2 = 0.41, p = 0.04).

The density of SNB1-(+) puncta in control group also correlated to short-term memory score (see Figures S6B and S6C). No significant correlation between density of presynaptic puncta and memory score was found in MgT-treated group. This lack of correlation is expected since MgT treatment reduced interindividual variation of memory score within the group (Figure 8D).

Altogether, these data suggest that increasing the density of synaptophysin-/synaptobrevin-containing presynaptic boutons might be a key structural change underlying the MgT-induced memory enhancement.

DISCUSSION

We found that increasing brain Mg^{2+} in both young and aged rats can enhance different forms of learning and memory (Figures 1, 2, and 3). Chronic MgT treatment upregulated NR2B-containing NMDAR and increased activation/expression of downstream signaling molecules in the hippocampus (Figure 4). This was associated with a dramatic increase in short-term synaptic facilitation and long-term potentiation that are critical for learning and memory (Figure 5). At the cellular level, on the other hand, MgT treatment also increased number of synaptophysin-/synaptobrevin-containing presynaptic boutons (Figure 6). Therefore, elevated Mg^{2+} induced reconfiguration of synaptic networks from a small number of synapses with high release probability to a larger number of synapses with low release probability (Figure 7). Finally, increase in the density of synaptophysin-/ synaptobrevin-containing presynaptic boutons correlated with improvement of memory functions (Figure 8).

What are the potential molecular mechanisms translating increase in brain Mg^{2+} level to enhancement of learning and memory? One molecular target of brain Mg^{2+} might be the NMDAR. NMDAR-dependent signaling plays a critical role in synaptic plasticity and memory (Martin et al., 2000; Nakazawa et al., 2004). Increase in NR2B-containing NMDAR via overexpression (Tang et al., 1999), augmentation of its membrane transportation (Wong et al., 2002), or reduction of its degradation (Hawasli et al., 2007) leads to enhancement of synaptic plasticity and learning and memory (for review, see Lee and Silva, 2009). In this study, we show that NR2B-containing NMDAR can be upregulated by increase in $[Mg^{2+}]_o$ in vitro and elevating brain Mg^{2+} in vivo. Our biophysical studies suggest that this upregulation might be due to a homeostatic regulatory mechanism (Figures 4A and 4B) (also see Turrigiano, 2008), which increases synaptic NMDAR to counterbalance the increase in blockage of NMDAR opening associated with chronic increase in $[Mg^{2+}]_o$. Under this condition, level of background NMDAR currents remains constant, but NMDAR current during bursting activity is enhanced.

One important effector downstream of NMDAR signaling is CaMKII. Increased activation of CaMKII was shown to underlie the enhancement of LTP and learning and memory observed in mice lacking the nociceptin opioid receptor (Mamiya et al., 2003; Manabe et al., 1998). In MgT-treated rats, upregulation of NR2B is associated with enhancement of CaMKII activation following memory task, suggesting that NMDAR signaling is enhanced. CREB is another important downstream molecule critical for learning and memory. Ca^{2+} influx through synaptic NMDAR triggers activation of CREB transcription factor, leading to the expression of genes that promote cell survival and synaptic plasticity such as the neurotrophic factor BDNF (Vanhoutte and Bading, 2003). Increased activation of CREB and/or expression of BDNF enhance LTP in hippocampus and learning and memory (Fukushima et al., 2008; Pang and Lu, 2004). Here, we found increased activation of CREB and higher level of BDNF in MgT-treated rats too. Because CREB can also be activated by other molecular pathways such as cAMP pathway (Silva et al., 1998), we cannot exclude the possibility that Mg^{2+} enhances CREB activation by acting on other signaling pathways.

In addition to voltage-dependent inhibition of NMDAR, Mg^{2+} may act at other targets that, synergistically or independently, might have led to the observed effects. For instance, in the intracellular compartment, an increase in Mg^{2+} could compete with Ca^{2+}, altering Ca^{2+} signaling. Furthermore, increased intracellular Mg^{2+} might influence Mg^{2+}-dependent enzymatic reactions, which might affect other cellular processes such as cell excitability and/or cell metabolism that might contribute to the observed enhancement of memory.

At the cellular level, we hypothesize that increase in bouton density might be a key change underlying memory enhancement by MgT. In support of this hypothesis, on one hand, is the temporal correlation among the onset of MgT treatment, elevation of brain Mg^{2+}, increase in density of synaptic boutons, and enhancement of memory functions (12 days time-course, Figures 1, 2 and 8). On the other hand, ending of MgT supplementation leads to a reduction in bouton density and memory performance back to the baseline in aged rats (Figures 2 and 8). Although changing extracellular $[Mg^{2+}]$ in vitro can alter synaptic configuration in hippocampal slices within 5 hr (Figure 7), slow time-course of Mg^{2+} loading into the brain (Figure 1A) might be the factor that delays the onset of MgT effect in vivo. In young rats the enhanced memory functions persisted for 60 days after the end of MgT treatment. This is possibly due to lower Mg^{2+} excretion rate in young animals (Corman and Michel, 1987). The exact mechanisms underlying the prolonged effect of MgT on memory functions in young rats remain to be investigated.

Diet, exercise, and environmental enrichment can affect brain health and cognitive function (for review, see Gómez-Pinilla, 2008). Here, we introduce a new strategy to enhance learning and memory and prevent age-related memory decline by increasing brain Mg^{2+}. It is worth noting that the control rats in the present study had a normal diet, which is widely accepted as containing a sufficient amount of Mg^{2+}. The effects we observed were due to elevation of body Mg^{2+} content to higher levels than a normal diet. Improvement of memory functions in aged rats by a high dosage of Mg^{2+} diet (2% elemental Mg^{2+}) has been reported before (Landfield and Morgan, 1984). However, it triggered weight loss due to Mg^{2+}-induced diarrhea, hindering further mechanistic studies. Having studied the biophysical effects of Mg^{2+} on synaptic plasticity in cultured hippocampal neurons in vitro (Slutsky et al., 2004), and after studying the homeostatic regulation of Mg^{2+} in intact rats, we concluded that development of a new compound that efficiently loads Mg^{2+} into the brain was essential. With this Mg^{2+} compound (MgT), we are able to study the influences of long-term elevation of brain magnesium on cognitive functions without

disrupting other physiological functions. In the current study, we did not test the effects of Mg^{2+} deficiency on synaptic plasticity and memory function. A previous study already showed that chronic reduction of dietary magnesium impairs memory (Bardgett et al., 2005). However, because Mg^{2+} is an essential ion for normal cellular functions and body health, many physiological functions are impaired with the reduction of body Mg^{2+}. Therefore, it is difficult to establish a casual relationship between brain Mg^{2+} and memory functions by induction of Mg^{2+} deficiency. Nonetheless, our "on/off" experiments in the T-maze provide evidence for the possible causal relationship between high Mg^{2+} intake and memory enhancement in aged rats (Figure 2D).

A recent survey indicates that a significant portion of the human population in industrialized countries do not take in a sufficient amount of Mg^{2+}. For example, only 32% of Americans met the RDA-DRI criteria for daily Mg^{2+} intake (http://www.ars.usda.gov/Services/docs.htm?docid=11046). Furthermore, Mg^{2+} intake in the aging population declines to 50% of the RDA (Ford and Mokdad, 2003). One might speculate that inadequate Mg^{2+} intake might impair cognitive function and lead to faster deterioration of memory during aging in human. Based on the data presented here, further studies to investigate the relationship between dietary Mg^{2+} intake, body, and brain Mg^{2+} status and cognitive abilities in human are warranted.

EXPERIMENTAL PROCEDURES

Rats for In Vivo Studies

Male Sprague-Dawley young (2-month-old), aging (12- to 18-month-olds), and aged (22- to 24-month-olds) rats were obtained from Vital River Laboratory (Animal Technology Co. Ltd., Beijing, China) and Charles River Laboratories (Boston). All rats were individually housed with free access to food and water under a 12:12 hr reversed light-dark cycle, with light onset at 8:00 p.m. All experiments involving animals were approved by Massachusetts Institute of Technology, Tsinghua University, and University of Toronto Committees on Animal Care.

Magnesium Compounds

The following magnesium preparations were used in the present study: magnesium-L-threonate (Magceutics Inc., USA), magnesium chloride (Modern Eastern Fine Chemicals, China), magnesium gluconate, and magnesium citrate (Sigma-Aldrich, Germany).

Magnesium-L-Threonate Treatment

Magnesium-L-threonate (604 mg/kg/day) was administered via drinking water (50 mg/kg/day elemental Mg^{2+}). The average drinking water per day was determined (~30 ml/day), and the dose was dissolved in the daily drinking amount. Rat chow contained 0.15% of elemental Mg^{2+}. We also monitored the food intake to determine the amount of Mg^{2+} intake from food.

Magnesium Content in the Cerebrospinal Fluid

The content of magnesium ion in cerebrospinal fluid (CSF) was estimated at baseline (day 0), 12, and 24 days of treatment with different magnesium preparations. Rats were treated with different magnesium preparations via drinking water (dose, 50 mg/kg/day elemental magnesium). Before each sampling point, rats were anesthetized with Chloral hydrate (400 mg/kg, i.p.) and then the CSF was manually obtained from the cisterna magna by the interruption of the atlanto-occipital membrane using a microneedle (diameter 450 μm). CSF samples (50–100 μl/rat) were collected and stored at −20°C until magnesium measurement was performed. Magnesium level in CSF was determined by Calmagite chromometry (Abernethy and Fowler, 1982).

Western Blot and ELISA Analyses

Samples of hippocampal homogenate from MgT-treated and control rats were resolved on polyacrylamide gels. Protein was then transferred to PVDF membrane and probed with anti-NR1 (Chemicon), NR2A (Upstate), NR2B (Santa Cruz Biotech), P-CaMKII, CaMKII, P-CREB, CREB, and β-actin (Cell signaling) antibodies followed by the appropriate HRP-coupled secondary antibody in Tris-buffered saline (pH 7.3) containing 5% dry milk and 0.1% Tween (BioRad). Visualization of immunoreactive bands was induced by enhanced chemiluminescence (Perkin Elmer Biosciences) captured on autoradiography film (Kodak Scientific). Standard curves were constructed to establish that we operated within the linear range of the chemiluminescence detection method. For the western blot analyses, digital images were quantified using GelPro Analyzer 3.1 software. The integrated optical density (IOD) of each immunoreactive band was measured. IOD was normalized to the IOD of actin band also in the same lane. Analysis of BDNF level in total homogenate of hippocampus was performed using Chemikine BDNF ELISA kit (Millipore) with complete adherence to manufacturer's instructions.

Slice Preparation

Coronal slices of the hippocampus (300 μm thick) were prepared (Wei et al., 2002) from 12-month-old rats (control and MgT-treated; Figure 5) and young rats (2 months old; Figure 7). Slices were transferred to a submerged recovery chamber containing oxygenated (95% O_2 and 5% CO_2) artificial cerebrospinal fluid (ACSF, mM): 124 NaCl, 2.5 KCl, 1.2 $CaCl_2$, 25 $NaHCO_3$, 1 NaH_2PO_4, 10 glucose. $[Mg^{2+}]_o$ was varied according to the experimental conditions. For experiments in Figure 5, slices were incubated in ACSF ($[Mg^{2+}]_o$ was matched to $[Mg^{2+}]_{CSF}$ in each group [1.06 to 1.2 mM]) at room temperature for 1 hr before recordings. For experiments presented in Figure 7, slices prepared from 2-month-old rats were preincubated at 32°C for 5 hr in two chambers containing ACSF with 0.8 and 1.2 mM $[Mg^{2+}]_o$, respectively, before recordings were performed.

Whole-Cell Recordings In Slice

Experiments were performed in a recording chamber on the stage of an Axioskop 2FS microscope with infrared DIC optics for visualizing whole-cell patch-clamp recordings. EPSCs were recorded from CA1 pyramidal neurons using an Axon 200B amplifier (Molecular Devices, Union City, CA), and stimulations were evoked in Schaffer collateral-commissural pathway. These procedures are described in detail in Supplemental Experimental Procedures.

LTP Induction Protocol

The postsynaptic neurons were switched to current-clamp recording mode. LTP was induced by 15 trains of presynaptic stimuli coupled with 15 trains of postsynaptic action potentials (ISI = 33 ms, inter-burst-interval = 5 s for both pre- and postsynaptic trains) delivered 10 ms after the onset of each EPSP. After that, recording was switched back to voltage-clamp mode.

Tissue Preparation and Fluorescent Immunostaining

Rats were anesthetized with Chloral hydrate and perfused transcardially with PBS, followed by 4% paraformaldehyde. The brain was postfixed in 4% paraformaldehyde for 24 hr before being transferred to 30% sucrose in PBS and left for 48 hr. Coronal sections from the hippocampus were cut at 5 μm on a cryostat (Leica), immediately mounted on superfrost slides, and left to dry overnight. On the following day, anatomically matched cryosections were washed with PBS and blocked (3% rabbit serum, 0.2% TX-100 in PBS) for 2 hr at 4°C. Sections were incubated with mouse anti-synaptophysin or anti-synaptobrevin antibody (Chemicon) in blocking solution for 24 hr at 4°C. On the second day, brain sections were rinsed with PBS and incubated with Alexa 488-coupled rabbit anti-mouse IgG in PBS (Invitrogen) for 2 hr at room temperature. Slides were then coverslipped with fluorescent mounting medium (Vector Laboratories) and left for 48 hr at 4°C.

Estimation of Density of Syn-/SNB1-(+) Puncta

Slides were coded until the completion of data analysis. Stained brain sections were imaged with Olympus IX-70 confocal microscope and Syn-/SNB1-(+) puncta were estimated using Image Pro-Plus software (Media Cybernetics). These procedures are described in detail in Supplemental Experimental Procedures.

Novel Object Recognition Test

The novel object recognition test was used as described before with modifications (Ennaceur and Delacour, 1988). These procedures are described in detail in Supplemental Experimental Procedures.

Elevated T-Maze

Spatial working memory was assessed using a T-maze non-matching-to-place task. These procedures are described in detail in Supplemental Experimental Procedures.

Morris Water Maze

The standard Morris water maze procedure was used with minor modifications (Morris, 1984). These procedures are described in detail in Supplemental Experimental Procedures.

Statistical Analysis

Data are presented as mean ± SEM (standard error of the mean). Statistical significance was defined as $p < 0.05$.

SUPPLEMENTAL INFORMATION

The Supplemental Information includes six figures, one table, and Supplemental Experimental Procedures and can be found with this article online at doi:10.1016/j.neuron.2009.12.026.

ACKNOWLEDGMENTS

We thank J. Feldman and D. Johnston for comments on the manuscript. This work was supported by grants from the National Institutes of Health NS37342, USA (to G.L.), National Basic Research Program of China Grants 2006CB3031 and 2009CB941303 (to G.L.), NSFC China 30630026 (to G.L.), The National High Technology Research and Development Program of China 2007AA02Z443 (to G.L.), Tsinghua-Yue-Yuen Medical Sciences Fund (to G.L.), China Scientific Foundation Grant for post doc 023205002 (to N.A.), and the NSFC China 20091300830 (to N.A.). G.L. declares that he is a cofounder of Magceutics, a company whose goal is to develop drugs to treat age-dependent memory decline and Alzheimer's disease.

Accepted: December 18, 2009
Published: January 27, 2010

REFERENCES

Abernethy, M.H., and Fowler, R.T. (1982). Micellar improvement of the calmagite complexometric measurement of magnesium in plasma. Clin. Chem. *28*, 520–522.

Bardgett, M.E., Schultheis, P.J., McGill, D.L., Richmond, R.E., and Wagge, J.R. (2005). Magnesium deficiency impairs fear conditioning in mice. Brain Res. *1038*, 100–106.

Barnes, C.A. (1979). Memory deficits associated with senescence: a neurophysiological and behavioral study in the rat. J. Comp. Physiol. Psychol. *93*, 74–104.

Bi, G.Q., and Poo, M.M. (1998). Synaptic modifications in cultured hippocampal neurons: dependence on spike timing, synaptic strength, and postsynaptic cell type. J. Neurosci. *18*, 10464–10472.

Burke, S.N., and Barnes, C.A. (2006). Neural plasticity in the ageing brain. Nat. Rev. Neurosci. *7*, 30–40.

Chen, K.S., Masliah, E., Mallory, M., and Gage, F.H. (1995). Synaptic loss in cognitively impaired aged rats is ameliorated by chronic human nerve growth factor infusion. Neuroscience *68*, 19–27.

Clements, J.D. (2003). Variance-mean analysis: a simple and reliable approach for investigating synaptic transmission and modulation. J. Neurosci. Methods *130*, 115–125.

Corman, B., and Michel, J.B. (1987). Glomerular filtration, renal blood flow, and solute excretion in conscious aging rats. Am. J. Physiol. *253*, R555–R560.

Diano, S., Farr, S.A., Benoit, S.C., McNay, E.C., da Silva, I., Horvath, B., Gaskin, F.S., Nonaka, N., Jaeger, L.B., Banks, W.A., et al. (2006). Ghrelin controls hippocampal spine synapse density and memory performance. Nat. Neurosci. *9*, 381–388.

Dudchenko, P.A. (2001). How do animals actually solve the T maze? Behav. Neurosci. *115*, 850–860.

Ennaceur, A., and Delacour, J. (1988). A new one-trial test for neurobiological studies of memory in rats. 1: Behavioral data. Behav. Brain Res. *31*, 47–59.

Ford, E.S., and Mokdad, A.H. (2003). Dietary magnesium intake in a national sample of US adults. J. Nutr. *133*, 2879–2882.

Fukushima, H., Maeda, R., Suzuki, R., Suzuki, A., Nomoto, M., Toyoda, H., Wu, L.J., Xu, H., Zhao, M.G., Ueda, K., et al. (2008). Upregulation of calcium/calmodulin-dependent protein kinase IV improves memory formation and rescues memory loss with aging. J. Neurosci. *28*, 9910–9919.

Gallagher, M., and Rapp, P.R. (1997). The use of animal models to study the effects of aging on cognition. Annu. Rev. Psychol. *48*, 339–370.

Geinisman, Y., Ganeshina, O., Yoshida, R., Berry, R.W., Disterhoft, J.F., and Gallagher, M. (2004). Aging, spatial learning, and total synapse number in the rat CA1 stratum radiatum. Neurobiol. Aging *25*, 407–416.

Gómez-Pinilla, F. (2008). Brain foods: the effects of nutrients on brain function. Nat. Rev. Neurosci. *9*, 568–578.

Hawasli, A.H., Benavides, D.R., Nguyen, C., Kansy, J.W., Hayashi, K., Chambon, P., Greengard, P., Powell, C.M., Cooper, D.C., and Bibb, J.A. (2007). Cyclin-dependent kinase 5 governs learning and synaptic plasticity via control of NMDAR degradation. Nat. Neurosci. *10*, 880–886.

Katz, B. (1969). The Release of Neural Transmitter Substances (Liverpool: Liverpool University Press).

Kim, Y.J., McFarlane, C., Warner, D.S., Baker, M.T., Choi, W.W., and Dexter, F. (1996). The effects of plasma and brain magnesium concentrations on lidocaine-induced seizures in the rat. Anesth. Analg. *83*, 1223–1228.

Landfield, P.W., and Morgan, G.A. (1984). Chronically elevating plasma Mg2+ improves hippocampal frequency potentiation and reversal learning in aged and young rats. Brain Res. *322*, 167–171.

Lee, Y.S., and Silva, A.J. (2009). The molecular and cellular biology of enhanced cognition. Nat. Rev. Neurosci. *10*, 126–140.

Li, C., Brake, W.G., Romeo, R.D., Dunlop, J.C., Gordon, M., Buzescu, R., Magarinos, A.M., Allen, P.B., Greengard, P., Luine, V., and McEwen, B.S. (2004). Estrogen alters hippocampal dendritic spine shape and enhances synaptic protein immunoreactivity and spatial memory in female mice. Proc. Natl. Acad. Sci. USA *101*, 2185–2190.

Lichtenwalner, R.J., Forbes, M.E., Bennett, S.A., Lynch, C.D., Sonntag, W.E., and Riddle, D.R. (2001). Intracerebroventricular infusion of insulin-like growth factor-I ameliorates the age-related decline in hippocampal neurogenesis. Neuroscience *107*, 603–613.

Malinow, R., and Tsien, R.W. (1990). Presynaptic enhancement shown by whole-cell recordings of long-term potentiation in hippocampal slices. Nature *346*, 177–180.

Mamiya, T., Yamada, K., Miyamoto, Y., König, N., Watanabe, Y., Noda, Y., and Nabeshima, T. (2003). Neuronal mechanism of nociceptin-induced modulation of learning and memory: involvement of N-methyl-D-aspartate receptors. Mol. Psychiatry *8*, 752–765.

Manabe, T., Noda, Y., Mamiya, T., Katagiri, H., Houtani, T., Nishi, M., Noda, T., Takahashi, T., Sugimoto, T., Nabeshima, T., and Takeshima, H. (1998). Facilitation of long-term potentiation and memory in mice lacking nociceptin receptors. Nature *394*, 577–581.

Markram, H., Lübke, J., Frotscher, M., and Sakmann, B. (1997). Regulation of synaptic efficacy by coincidence of postsynaptic APs and EPSPs. Science *275*, 213–215.

Martin, S.J., Grimwood, P.D., and Morris, R.G. (2000). Synaptic plasticity and memory: an evaluation of the hypothesis. Annu. Rev. Neurosci. *23*, 649–711.

Mayer, M.L., Westbrook, G.L., and Guthrie, P.B. (1984). Voltage-dependent block by Mg2+ of NMDA responses in spinal cord neurones. Nature *309*, 261–263.

McKee, J.A., Brewer, R.P., Macy, G.E., Phillips-Bute, B., Campbell, K.A., Borel, C.O., Reynolds, J.D., and Warner, D.S. (2005). Analysis of the brain bioavailability of peripherally administered magnesium sulfate: A study in humans with acute brain injury undergoing prolonged induced hypermagnesemia. Crit. Care Med. *33*, 661–666.

Morris, R. (1984). Developments of a water-maze procedure for studying spatial learning in the rat. J. Neurosci. Methods *11*, 47–60.

Morris, R.G., Anderson, E., Lynch, G.S., and Baudry, M. (1986). Selective impairment of learning and blockade of long-term potentiation by an N-methyl-D-aspartate receptor antagonist, AP5. Nature *319*, 774–776.

Murnick, J.G., Dubé, G., Krupa, B., and Liu, G. (2002). High-resolution iontophoresis for single-synapse stimulation. J. Neurosci. Methods *116*, 65–75.

Nakazawa, K., McHugh, T.J., Wilson, M.A., and Tonegawa, S. (2004). NMDA receptors, place cells and hippocampal spatial memory. Nat. Rev. Neurosci. *5*, 361–372.

Nowak, L., Bregestovski, P., Ascher, P., Herbet, A., and Prochiantz, A. (1984). Magnesium gates glutamate-activated channels in mouse central neurones. Nature *307*, 462–465.

O'Kusky, J.R., Ye, P., and D'Ercole, A.J. (2000). Insulin-like growth factor-I promotes neurogenesis and synaptogenesis in the hippocampal dentate gyrus during postnatal development. J. Neurosci. *20*, 8435–8442.

Pang, P.T., and Lu, B. (2004). Regulation of late-phase LTP and long-term memory in normal and aging hippocampus: role of secreted proteins tPA and BDNF. Ageing Res. Rev. *3*, 407–430.

Schiavo, G., Benfenati, F., Poulain, B., Rossetto, O., Polverino de Laureto, P., DasGupta, B.R., and Montecucco, C. (1992). Tetanus and botulinum-B neurotoxins block neurotransmitter release by proteolytic cleavage of synaptobrevin. Nature *359*, 832–835.

Silva, A.J., Kogan, J.H., Frankland, P.W., and Kida, S. (1998). CREB and memory. Annu. Rev. Neurosci. *21*, 127–148.

Silver, R.A. (2003). Estimation of nonuniform quantal parameters with multiple-probability fluctuation analysis: theory, application and limitations. J. Neurosci. Methods *130*, 127–141.

Slutsky, I., Sadeghpour, S., Li, B., and Liu, G. (2004). Enhancement of synaptic plasticity through chronically reduced Ca2+ flux during uncorrelated activity. Neuron *44*, 835–849.

Smith, T.D., Adams, M.M., Gallagher, M., Morrison, J.H., and Rapp, P.R. (2000). Circuit-specific alterations in hippocampal synaptophysin immunoreactivity predict spatial learning impairment in aged rats. J. Neurosci. *20*, 6587–6593.

Tang, Y.P., Shimizu, E., Dube, G.R., Rampon, C., Kerchner, G.A., Zhuo, M., Liu, G., and Tsien, J.Z. (1999). Genetic enhancement of learning and memory in mice. Nature *401*, 63–69.

Turrigiano, G.G. (2008). The self-tuning neuron: synaptic scaling of excitatory synapses. Cell *135*, 422–435.

Vanhoutte, P., and Bading, H. (2003). Opposing roles of synaptic and extrasynaptic NMDA receptors in neuronal calcium signalling and BDNF gene regulation. Curr. Opin. Neurobiol. *13*, 366–371.

Vicario-Abejón, C., Owens, D., McKay, R., and Segal, M. (2002). Role of neurotrophins in central synapse formation and stabilization. Nat. Rev. Neurosci. *3*, 965–974.

Wei, F., Qiu, C.S., Kim, S.J., Muglia, L., Maas, J.W., Pineda, V.V., Xu, H.M., Chen, Z.F., Storm, D.R., Muglia, L.J., and Zhuo, M. (2002). Genetic elimination of behavioral sensitization in mice lacking calmodulin-stimulated adenylyl cyclases. Neuron *36*, 713–726.

Williams, K. (1993). Ifenprodil discriminates subtypes of the N-methyl-D-aspartate receptor: selectivity and mechanisms at recombinant heteromeric receptors. Mol. Pharmacol. *44*, 851–859.

Williams, S.R., and Mitchell, S.J. (2008). Direct measurement of somatic voltage clamp errors in central neurons. Nat. Neurosci. *11*, 790–798.

Wilson, I.A., Gallagher, M., Eichenbaum, H., and Tanila, H. (2006). Neurocognitive aging: prior memories hinder new hippocampal encoding. Trends Neurosci. *29*, 662–670.

Wong, R.W., Setou, M., Teng, J., Takei, Y., and Hirokawa, N. (2002). Overexpression of motor protein KIF17 enhances spatial and working memory in transgenic mice. Proc. Natl. Acad. Sci. USA *99*, 14500–14505.

Zucker, R.S., and Regehr, W.G. (2002). Short-term synaptic plasticity. Annu. Rev. Physiol. *64*, 355–405.